DEEP LEARNING-BASED DETECTION OF AGRICULTURAL BURNED AREAS USING TRUE COLOR SATELLITE IMAGERY

Worawit SUPPAWIMUT [1,2] **&** ***Ratchaphon SAMPHUTTHANONT*** [1,2*]

DOI: 10.21163/GT_2026.212.09

ABSTRACT

Chiang Mai Province, situated in northern Thailand, is experiencing persistent challenges regarding seasonal haze and particulate matter (PM2.5) contamination. The primary sources of these emissions are agricultural burning practices, particularly the combustion of rice straw and stubble in proximity to residential areas. This study aims to (1) assess agricultural burned areas in rice fields using the differenced Normalized Burn Ratio (dNBR) derived from Sentinel-2 imagery, and (2) develop a deep learning model to detect burned areas from true color satellite imagery (RGB) using the U-Net architecture. Sentinel-2 Level-2A images acquired before and after burning events in 2024 were used for analysis. The study focused on rice cultivation areas, while clouds, cloud shadows, and water bodies were removed using the Scene Classification Layer. Subsequently, the Normalized Burn Ratio (NBR) and the Differenced Normalized Burn Ratio (dNBR) were calculated to generate a burned area mask. The validation results indicate that a dNBR threshold of ≥ 0.1 is appropriate for the specific context of the study area. This mask was used as reference data for training the deep learning model. The U-Net model was trained using RGB image tiles and corresponding binary masks, with the final deep learning dataset consisting of 2,560 image tiles of 256 × 256 pixels after data augmentation. A spatial hold-out strategy was applied to prevent spatial data leakage between training, validation and test datasets. The results show that U-Net outperformed DeepLabv3+, achieving an Intersection over Union (IoU) of 0.9292 and an F1-score of 0.9633, indicating strong capability in detecting small burned patches. Spatial analysis revealed that the burned areas accounted for 9.952% of the total image area and 18.937% of the total cultivated land. These findings suggest that integrating true-color satellite imagery with deep learning techniques provides significant potential for monitoring agricultural burning and supporting local strategies to mitigate PM2.5 pollution.

Keywords: *Deep Learning, Agricultural Burned Area, Normalized Burn Ratio, Satellite Imagery*

1. INTRODUCTION

Air pollution caused by fine particulate matter (PM2.5) has become a critical environmental and public health issue worldwide. In northern Thailand, particularly in Chiang Mai Province, recurrent haze episodes are strongly associated with open biomass burning occurring in both forest and agricultural areas. Among these sources, agricultural residue burning—especially rice straw burning—plays a significant role due to its proximity to urban and peri-urban communities. Previous studies have reported that rice residue burning can emit up to 38 ± 22 kilotons of PM2.5 annually, while populations in suburban areas experience higher exposure levels compared to those affected by distant forest fires (Junpen et al., 2018). Elevated PM2.5 concentrations have also been significantly associated with increased hospital admissions related to respiratory and cardiovascular diseases, particularly in urban Chiang Mai (Kamton et al., 2019; Jarernwong et al., 2023). In addition, biomass burning emissions can be identified through chemical tracers such as potassium, which serves as a key indicator of biomass combustion in the atmosphere (Khamkaew et al., 2016).

[1] *Department of Geography and Geoinformatics, Faculty of Humanities and Social Sciences, Chiang Mai Rajabhat University, Thailand, worawit_sup@cmru.ac.th (WS), corresponding author* [*] *ratchaphon_sam@cmru.ac.th (RS).*

[2] *Asian Air Quality Operations Center by Space Technology, Geoinformatics & Environmental Engineering (AiroTEC), Chiang Mai Rajabhat University, Thailand.*

At the global scale, biomass burning represents a major source of atmospheric pollutants, contributing significantly to emissions of carbonaceous aerosols and trace gases such as CO and NO_x (Andreae, 2019). It has been estimated that biomass burning releases approximately 2.2 Pg C yr^{-1}, with a substantial portion originating from small fires that are often underestimated in conventional emission inventories (van der Werf et al., 2017). Regionally, Southeast Asia is recognized as one of the most complex aerosol environments, where seasonal haze is driven by interactions among emission sources, meteorological conditions, and land-use dynamics (Reid et al., 2013). These haze events frequently result in severe air pollution episodes across the region, posing substantial health risks, as exposure to PM2.5 has been linked to increased mortality and a wide range of cardiopulmonary diseases even at relatively low concentrations (World Health Organization, 2021).

Despite continuous regulatory efforts, agricultural burning in Chiang Mai remains prevalent, particularly during the post-harvest period of rice cultivation. These burning activities typically occur between November and December and are characterized by small, fragmented patches distributed across agricultural fields near populated areas. Such spatial characteristics contribute to rapid increases in local PM2.5 concentrations, emphasizing the importance of accurately detecting and monitoring burned areas at fine spatial scales.

Satellite remote sensing has been widely applied for monitoring biomass burning at regional and global scales. Burned area products derived from Moderate Resolution Imaging Spectroradiometer (MODIS), such as MCD64A1, provide long-term and consistent global datasets at moderate spatial resolution (~500 m) by integrating surface reflectance time series with active fire detections (Giglio et al., 2018). Similarly, the Visible Infrared Imaging Radiometer Suite (VIIRS) enhances fire detection capability through improved spatial resolution (375 m), allowing better identification of small and low-intensity fires (Schroeder et al., 2014). However, both MODIS and VIIRS remain limited in detecting small and fragmented agricultural burning due to their coarse spatial resolution, leading to potential underestimation of burned areas in smallholder agricultural systems.

The availability of higher-resolution satellite data, such as Landsat and Sentinel-2 (10–20 m), has significantly improved the detection of small burned areas. Sentinel-2, in particular, enables the calculation of spectral indices such as the Normalized Burn Ratio (NBR) and differenced NBR (dNBR), which are widely used for burned area detection and burn severity assessment. Previous studies have demonstrated that Sentinel-2 can detect small-scale agricultural burning that is often missed by traditional hotspot data (Chuvieco & Stoyanov, 2023). Furthermore, multi-temporal approaches integrating Sentinel-2 data have shown improved accuracy in capturing small burned patches, especially those smaller than 100 hectares (Roteta et al., 2019). In the context of Chiang Mai, Samphutthanont (2024) demonstrated that dNBR derived from Sentinel-2 can effectively detect burned areas in rice fields characterized by low fuel loads and low combustion temperatures, which are typically undetectable using conventional hotspot data. Nevertheless, these approaches rely heavily on spectral index calculations and often require multiple processing steps.

Recent advances in deep learning have significantly transformed remote sensing image analysis, particularly for semantic segmentation tasks. Convolutional Neural Networks (CNNs), including Fully Convolutional Networks (Long et al., 2015) and U-Net architectures (Ronneberger et al., 2015), enable pixel-level classification by learning complex spatial features directly from imagery. These approaches have demonstrated superior performance compared to traditional machine learning methods, particularly in large-scale image analysis (Ma et al., 2019; Zhu et al., 2017). In the context of burned area detection, deep learning models have shown strong capability in capturing spatial patterns of burned regions, especially when applied to high-resolution satellite imagery (Knopp et al., 2020; Martins et al., 2022; Hu et al., 2021). For example, CNN-based models applied to Sentinel-2 data have achieved overall accuracies exceeding 97% and have outperformed conventional machine learning approaches (Tonbul et al., 2023). Moreover, integrating True Color (RGB) imagery with spectral indices has been shown to further improve model performance (Yılmaz & Kavzoğlu, 2024).

However, most existing studies rely on multispectral inputs and spectral indices as primary features. Research focusing on the direct detection of agricultural burned areas using only True Color (RGB) satellite imagery remains limited. This limitation is particularly relevant in regions such as

northern Thailand, where agricultural burning occurs in small, fragmented patches within complex urban–rural landscapes and directly impacts human health. This gap highlights the need for developing flexible, data-driven approaches that can operate effectively using readily interpretable imagery and support practical applications in environmental monitoring and policy decision-making.

Therefore, the objectives of this study are to (1) assess agricultural burned areas in rice fields using the differenced Normalized Burn Ratio (dNBR), and (2) develop and evaluate a deep learning-based approach for detecting agricultural burned areas in rice fields from true color satellite imagery in Chiang Mai Province, Thailand. The findings are expected to support improved monitoring of PM2.5 emission sources and contribute to more effective haze management strategies at the local level.

2. STUDY AREA

The study area for this research encompasses the provincial boundaries of Chiang Mai Province in northern Thailand, covering a total area of 22,436.07 square kilometers. This region includes approximately 5,519.08 square kilometers of agricultural land, accounting for 24.60% of the total provincial area (Office of the Permanent Secretary for Agriculture and Cooperatives, Chiang Mai Province, 2026), where agricultural burning activities remain prevalent.

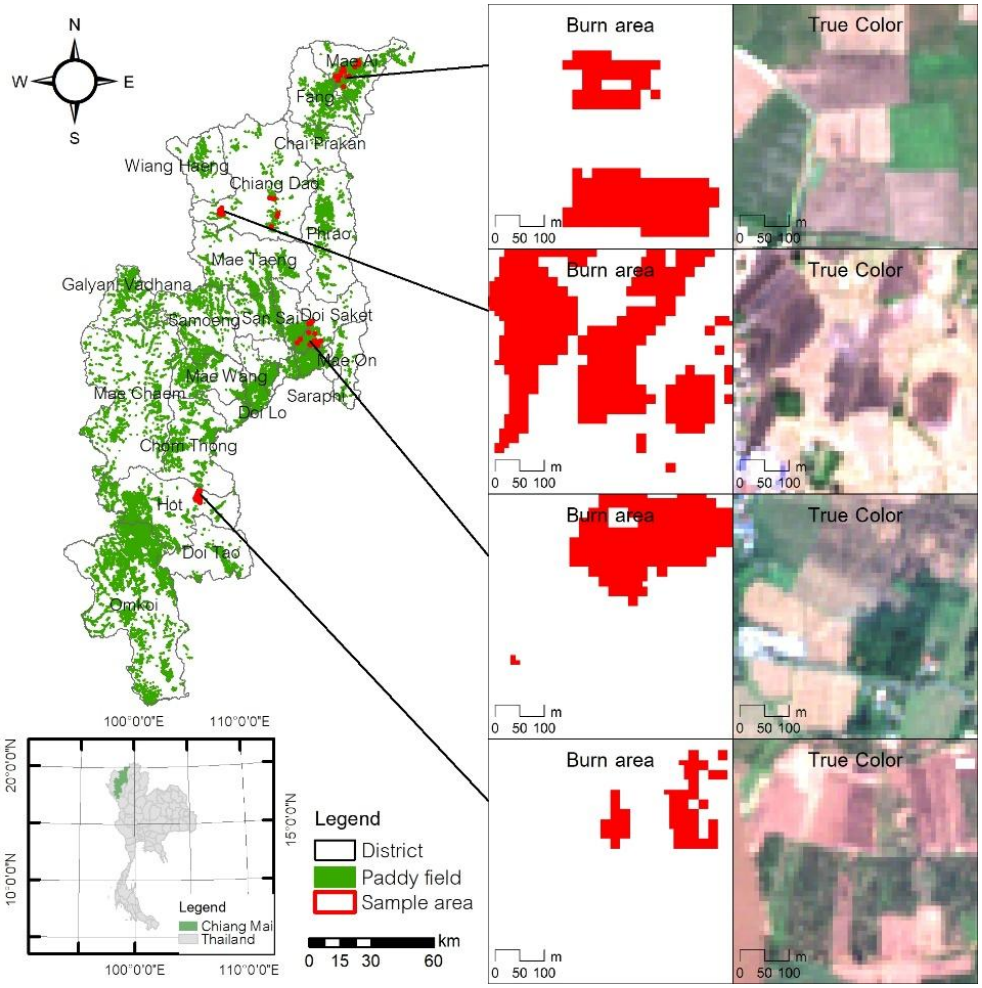

Fig. 1. Study area in Chiang Mai Province, Thailand, showing the selected districts used to generate the training dataset, the distribution of agricultural burned areas, and examples of true color satellite imagery (RGB) in four districts.

To develop representative training datasets, four districts distributed across the northern, central, and southern parts of the province were selected as sample areas: Mae Ai District, Chiang Dao District, Doi Saket District, and Hot District. These districts were used to construct spatially distributed training datasets for the analysis. The study primarily focuses on detecting agricultural burned areas, particularly in rice cultivation fields, using the differenced Normalized Burn Ratio (dNBR) and deep learning techniques (**Fig. 1**).

3. DATA AND METHODS

The Data and Methods section begin with the presentation of the conceptual framework (**Fig. 2**) in which Input Data, Processing, dNBR Label generation, respectively, Deep Learning Model, Model Evaluation are discussed, and if the accuracy assessment is satisfactory then the procedure ends with the final burned area map and other spatial analysis possibilities.

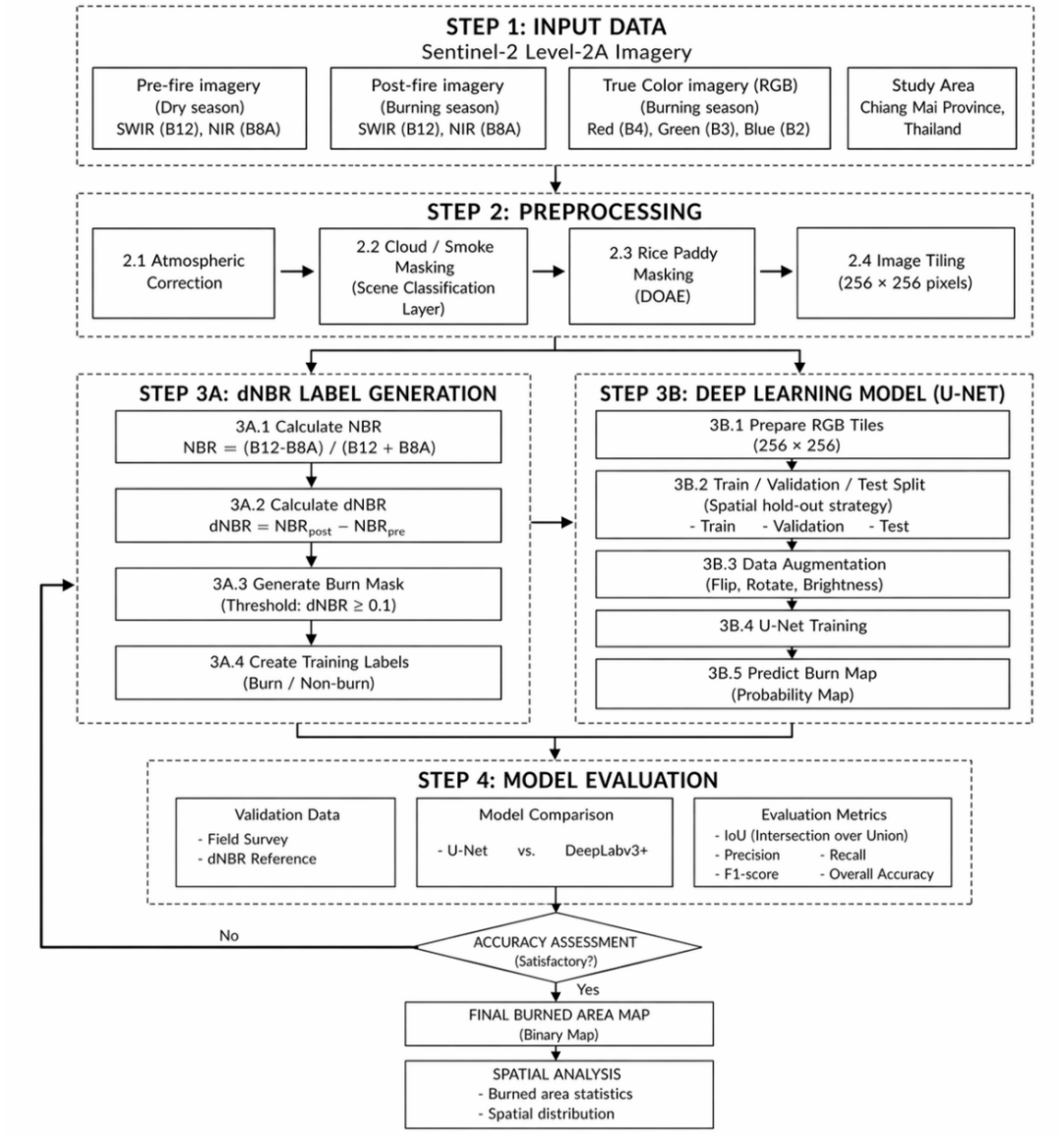

Fig. 2. Conceptual framework of the proposed methodology integrating spectral index-based analysis (dNBR) and deep learning (U-Net) for detecting agricultural burned areas from Sentinel-2 imagery.

3.1. Satellite Image Data Preparation

This study utilized Sentinel-2 Level-2A (L2A) satellite data, which provide atmospherically corrected surface reflectance products suitable for high-resolution analysis of land surface changes. In addition, areas obscured by smoke from biomass burning were identified and removed to minimize potential interference in the analysis. Data from the post-harvest period of rice cultivation in 2024 were specifically selected to encompass the intervals immediately before and after the burning of rice straw and stubble within the study area. The acquisition dates used for the analysis are summarized in **Table 1**.

For the calculation of the Normalized Burn Ratio (NBR), Sentinel-2 Level-2A imagery in the Short-Wave Infrared (SWIR) and Narrow Near-Infrared (NIR) bands was employed, both having a spatial resolution of 20 meters. Meanwhile, Sentinel-2 Level-2A imagery used for True Color Composite (RGB), consisting of Band 4 (Red), Band 3 (Green), and Band 2 (Blue), has a spatial resolution of 10 meters.

To ensure that the analysis focused specifically on the target area, all satellite imagery was clipped to include only rice cultivation areas using available agricultural field boundary data. This spatial masking process helps reduce noise caused by land cover changes in other land-use types, such as forested areas or built-up zones, thereby improving the accuracy of burned area detection within agricultural landscapes.

As clouds, cloud shadows, and water bodies may introduce significant uncertainty in spectral index calculations, this study utilized the Scene Classification Layer (SCL) provided with Sentinel-2 data to identify and remove these areas from the analysis. Only pixels classified as non-vegetated areas (SCL value = 5) were retained, while pixels corresponding to clouds, cloud shadows, and water were excluded. This preprocessing step helps reduce the likelihood of misclassifying non-burned areas as burned areas.

Subsequently, a dataset of 64 satellite images was prepared in True Color Composite (RGB) format using Band 4 (Red), Band 3 (Green), and Band 2 (Blue). These images were used both for visual interpretation and as input data for the deep learning analysis in the subsequent stage.

Table 1.

Sentinel-2 satellite images used for pre-fire and post-fire periods.

District	Pre-fire Date	Post-fire Date
Mae Ai District	30-Oct-24	4-Nov-24
Chiang Dao District	24-Nov-24	4-Dec-24
Doi Saket District	19-Nov-24	4-Dec-24
Hot District	30-Oct-24	4-Nov-24

The selection of Sentinel-2 satellite imagery was based on principles appropriate for burned area analysis. The acquisition dates were chosen to correspond with periods when agricultural burning was observed in the study area. These periods were identified through both field observations and visual interpretation of true color satellite imagery, which indicated that burning activities mainly occurred between November and December. Subsequently, satellite images acquired during this period that were free from obstructions such as clouds or smoke were selected to ensure reliable analysis of burned areas.

3.2. Burned Area Analysis Using the dNBR Index

Burned area detection in this study was based on the Normalized Burn Ratio (NBR), a spectral index developed to enhance the contrast between burned and unburned surfaces. The index was calculated using the reflectance values from the Short-Wave Infrared (SWIR) and Narrow Near-Infrared (Narrow NIR) bands of Sentinel-2 imagery, as expressed in Equation (1):

$$\mathrm{NBR} = \frac{\mathrm{B12} - \mathrm{B8A}}{\mathrm{B12} + \mathrm{B8A}} \quad (1)$$

where B12 and B8A represent the surface reflectance values of the SWIR and Narrow NIR bands, respectively.

Subsequently, the differenced Normalized Burn Ratio (dNBR) was calculated by subtracting the pre-fire NBR from the post-fire NBR in order to emphasize spectral changes caused by burning activities in rice paddy fields. The dNBR was computed as expressed in Equation (2):

$$\mathrm{dNBR} = \mathrm{NBR}_{\text{post-fire}} - \mathrm{NBR}_{\text{pre-fire}} \quad (2)$$

The resulting dNBR values were analyzed together with spatial data of sample rice fields. The analysis revealed that rice fields after harvesting or after the burning of rice residues tended to exhibit higher dNBR values. However, the burning severity in agricultural areas was generally lower than that typically observed in forest fires. In the study area, the maximum dNBR values were also found to be lower than the commonly used international threshold for burned area classification (e.g., 0.27 according to the USGS standard). This finding indicates the necessity of adjusting the classification threshold to better align with the specific characteristics of burned rice fields in the study area.

Several threshold levels were therefore tested based on the dNBR burn severity classification proposed by the United States Geological Survey (USGS), which categorizes burn severity into seven classes. In this study, areas classified as Moderate-low Severity with dNBR values greater than 0.1 ($\mathrm{dNBR} > 0.1$) were considered burned areas. This threshold was found to provide the most appropriate representation of actual burned areas in rice fields and showed strong agreement with visual interpretation derived from true color satellite imagery.

In addition, True Color satellite composite images were generated using the three visible bands of Sentinel-2 imagery, namely Band 4 (Red), Band 3 (Green), and Band 2 (Blue). These composites corresponded to the post-fire observation period, which was the same time frame used for the burned area classification described above.

The burned area classification results derived from the dNBR index together with the True Color satellite imagery were subsequently used as reference data (labels or ground truth) for training and evaluating the deep learning model in the next stage of the study.

To prepare the dataset for model training and evaluation, the burned area classification results from the dNBR analysis and the True Color satellite images were exported as JPEG image files. In this study, burned areas identified from the dNBR classification were visualized in red, while non-burned areas were represented in white. For the True Color composite images, the display settings were adjusted using Standard Deviation Stretch to enhance visual contrast.

The satellite image samples were extracted as square image patches, with 16 images selected from each district, covering the four study districts: Mae Ai, Chiang Dao, Doi Saket, and Hot. In total, 64 image samples were generated, consisting of 64 burned area masks and 64 corresponding True Color images. Each image patch represents an area of 500 × 500 meters at a map scale of 1:5,000, with a map layout size of 10 × 10 centimeters. The exported images were produced at a resolution of 602 pixels (153 dpi) for use in deep learning model training and evaluation.

In addition to the continuous dNBR values, burn severity can be categorized into discrete classes to facilitate interpretation and comparison across different areas. The classification framework widely adopted by the United States Geological Survey (USGS) is based on the Landscape Assessment (LA) methodology developed by Key and Benson (2006), which integrates remote sensing indices with field-based observations such as the Composite Burn Index (CBI). In this framework, burn severity is defined as the magnitude of ecological change caused by fire, rather than the intensity of the fire itself, emphasizing the post-fire effects on vegetation, soil, and ecosystem structure.

The USGS classification scheme uses dNBR values derived from pre- and post-fire NBR images to represent the degree of change caused by fire. These values are then stratified into several burn severity levels, typically including unburned, low, moderate-low, moderate-high, and high severity classes. This approach enables the spatial representation of fire effects across landscapes and allows for consistent comparison of burn severity across different regions and time periods (Key & Benson, 2006).

However, previous studies have highlighted limitations associated with using absolute dNBR thresholds across heterogeneous landscapes. Miller and Thode (2007) demonstrated that the magnitude of dNBR is strongly influenced by pre-fire vegetation conditions, which may lead to misclassification of burn severity when applying uniform thresholds. For example, areas with sparse vegetation may exhibit low dNBR values even after complete biomass loss, while densely vegetated areas may show high dNBR values under similar fire effects. This suggests that burn severity should be interpreted as a relative measure of ecological change rather than an absolute spectral difference.

To address this issue, Miller and Thode (2007) proposed the use of a relative version of dNBR (RdNBR), which normalizes the change relative to pre-fire conditions, thereby improving the comparability of burn severity across different vegetation types and landscapes. Although RdNBR provides advantages in heterogeneous environments, the conventional dNBR-based classification remains widely used due to its simplicity and operational applicability, particularly in large-scale assessments where field calibration data may be limited. In this study, the dNBR classification approach is adapted to the context of agricultural burning in rice paddy fields. Given the relatively low biomass and rapid post-harvest changes in these areas, the standard USGS thresholds may not be directly applicable. Therefore, an adjusted threshold ($dNBR > 0.1$) is employed to identify burned areas, ensuring that small-scale and low-intensity agricultural burns can be effectively detected while maintaining consistency with the conceptual framework of burn severity classification.

3.3. Deep Learning Analysis

This research employs a deep learning approach to develop a method for detecting agricultural burned areas from true color satellite imagery (RGB). The analysis focused on pixel-level segmentation in order to accurately delineate the boundaries of small burned patches commonly found in agricultural fields. The input data consisted of RGB image tiles with a size of 256×256 pixels, accompanied by binary masks (1 = burned area, 0 = other areas) for supervised learning.

To ensure robust model evaluation and avoid spatial autocorrelation, the dataset was divided into training, validation, and testing sets using a spatial hold-out strategy. This approach ensures that the performance metrics reflect the model's generalizability to unseen geographic areas. Prior to model training, several preprocessing steps were performed to standardize the data. These included resizing the images to a consistent dimension, normalizing pixel values to an appropriate range for model training, and conducting random quality checks to verify the correct alignment between input images and their corresponding masks.

The deep learning model used in this study was the U-Net architecture, which is widely recognized for its effectiveness in image segmentation tasks. The U-Net model is capable of capturing both global contextual information and fine spatial details through the use of skip connections that link encoder and decoder layers. Although advanced architectures such as Attention U-Net and ResU-Net have been proposed in recent studies, the standard U-Net was selected in this research due to its computational efficiency, architectural simplicity, and proven effectiveness in small dataset scenarios. These characteristics make it particularly suitable for practical implementation in local-scale applications and resource-constrained environments. The model output is a probability map representing the likelihood that each pixel belongs to a burned area. This probability map is subsequently converted into a binary mask for burned area estimation. To improve model robustness, data augmentation techniques were applied during training, including image flipping, rotation, and slight brightness adjustments. Model performance was continuously monitored using the validation dataset to identify the optimal model during training.

Model performance was evaluated using standard metrics that assess both classification accuracy and the capability of detecting burned areas. Additionally, the reliability of the results was assessed by comparing burned area detection from the U-Net model and the DeepLabv3+ model (using a True Color image acquired on 24 December 2024) with burned area classifications derived from field observations combined with dNBR analysis (using images from 4 and 24 December 2024 representing pre-fire and post-fire conditions, respectively). The comparison focused on a sample burned rice field area observed on 21 December 2024 in Doi Saket District, Chiang Mai Province, as illustrated in **Fig. 3**. Furthermore, a comparative analysis was performed to determine quantitative performance metrics, including Intersection over Union (IoU), Precision, Recall, F1-score, and Overall Accuracy, as presented in **Table 2**.

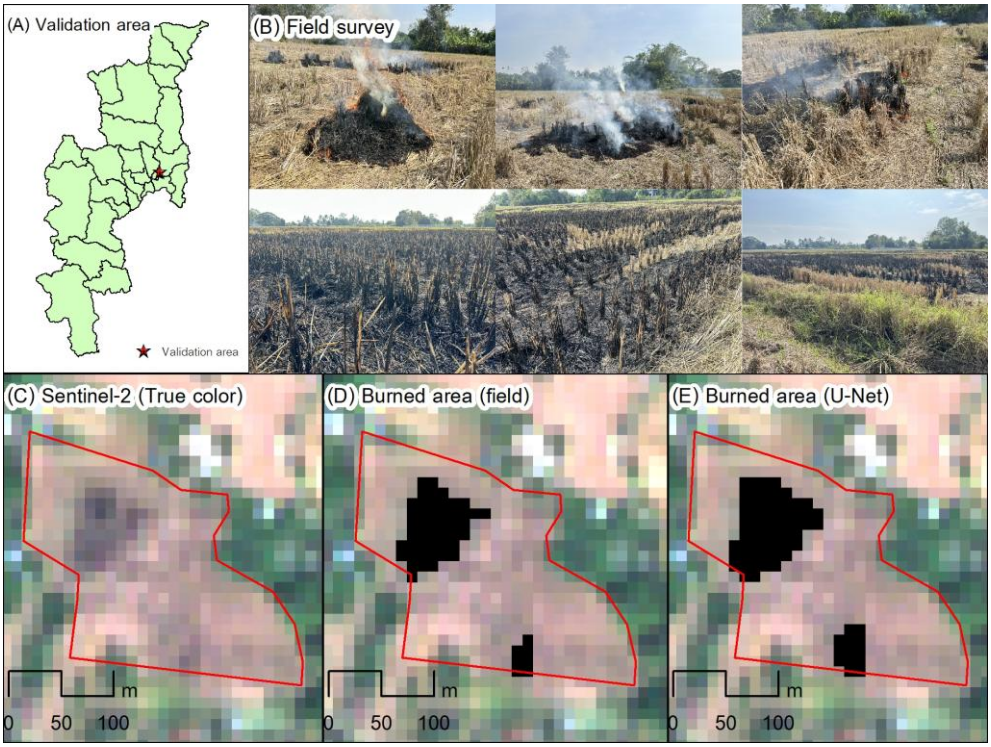

Fig. 3. Validation framework for burned area detection: (A) location of the study site, (B) field survey observations, (C) Sentinel-2 true color imagery, (D) reference burned area from field data, and (E) U-Net segmentation results in rice paddy fields, Doi Saket District, Chiang Mai Province, Thailand.

The deep learning dataset consisted of 2,560 samples, including RGB image tiles and their corresponding binary burn masks derived from Sentinel-2 True Color imagery. The original dataset was divided using a spatial hold-out strategy into training, validation, and test sets to reduce spatial data leakage and improve model generalization. Specifically, the training set contained 896 image tiles and 896 corresponding masks (70%), while the validation set included 256 image tiles and 256 masks (20%), and the test set consisted of 128 image tiles and 128 masks (10%).

To improve model robustness and increase sample diversity, data augmentation was applied only to the training dataset using three techniques: horizontal flipping, vertical flipping, and rotation. After augmentation, the total number of samples used in the deep learning analysis increased to 2,560.

The U-Net model was trained using the Adam optimizer due to its computational efficiency and stability in deep learning applications. The learning rate was set to 0.0001 to ensure stable convergence during training, and a batch size of 16 was used to balance computational efficiency and segmentation performance. To address class imbalance between burned and non-burned pixels, a

hybrid loss function combining Binary Cross-Entropy (BCE) and Dice loss was employed to improve the model's ability to accurately detect and delineate small burned areas. The model was trained for 100 epochs while monitoring both training and validation performance to reduce overfitting and ensure convergence.

4. RESULTS

4.1. Model Performance

The results of this study demonstrate that the U-Net model can effectively detect agricultural burned areas in rice paddies from true color satellite imagery (RGB), achieving high performance (IoU = 0.9292; F1-score = 0.9633). As presented in **Table 2**, the model outperformed DeepLabv3+ in the context of smallholder agricultural landscapes in Chiang Mai Province.

Table 2.

Quantitative performance metrics of the U-Net and DeepLabv3+ models.

Model	IoU	Precision	Recall	F1-score	Overall Accuracy
U-Net	0.9292	0.9292	0.9999	0.9633	0.9292
DeepLabv3+	0.8664	0.8664	0.9999	0.9284	0.8664

4.2. Training Behavior of the Model

The training results indicate that the training IoU increased rapidly during the early stages of training and gradually stabilized at a high level in the subsequent epochs, suggesting that the model was able to effectively learn the spatial patterns of burned areas from the training dataset (**Fig. 4**).

Meanwhile, the validation IoU showed a similar increasing trend during the initial training phase and then fluctuated within a relatively stable range throughout the training process. This behavior indicates that the model was capable of transferring the learned knowledge to unseen data, although some fluctuations occurred due to the class imbalance between burned and non-burned areas. For the graph on the right, the training loss decreased continuously and eventually converged, clearly demonstrating the convergence of the model during training.

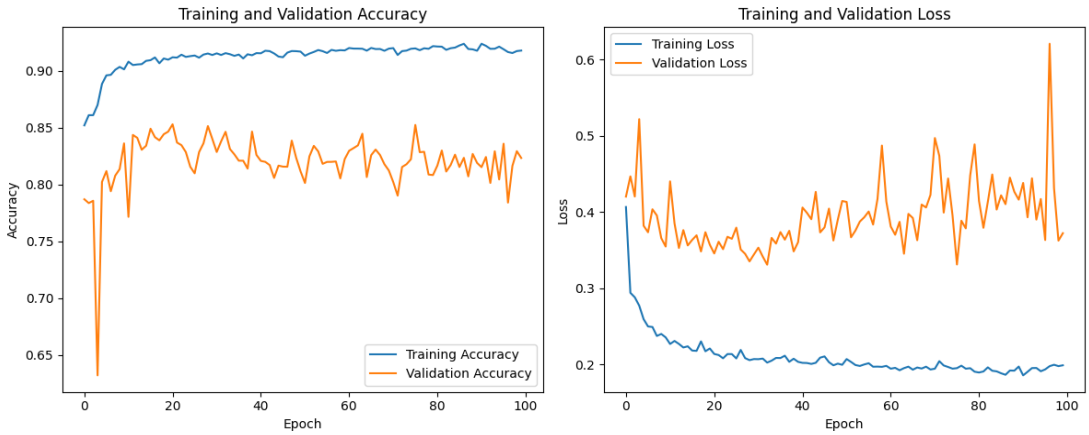

Fig. 4. Training and validation curves of the U-Net model over 100 epochs: Training IoU and Validation IoU (left), and Training loss and Validation loss (right).

In contrast, the validation loss decreased during the early stage and then fluctuated at a slightly higher level than the training loss, which is a common characteristic in spatial image segmentation tasks with imbalanced class distributions. Importantly, no consistent upward trend in validation loss was observed, indicating that the model did not exhibit severe overfitting during training.

Overall, the graphs presented in **Fig. 4** demonstrate that the developed U-Net model exhibited stable training behavior, effectively learned the spatial patterns of burned areas from true color satellite imagery, and showed good generalization capability for detecting burned areas in real agricultural landscapes.

4.3. Spatial Distribution of Agricultural Burning

The classification of burned areas within rice paddies were classified using the U-Net model in five selected locations where rice cultivation covered more than 50% of the area. These sites are distributed across rice-growing regions in Chiang Mai Province, Thailand. The analysis used Sentinel-2 True Color imagery acquired on 24 December 2024 as the input dataset (**Fig. 5**).

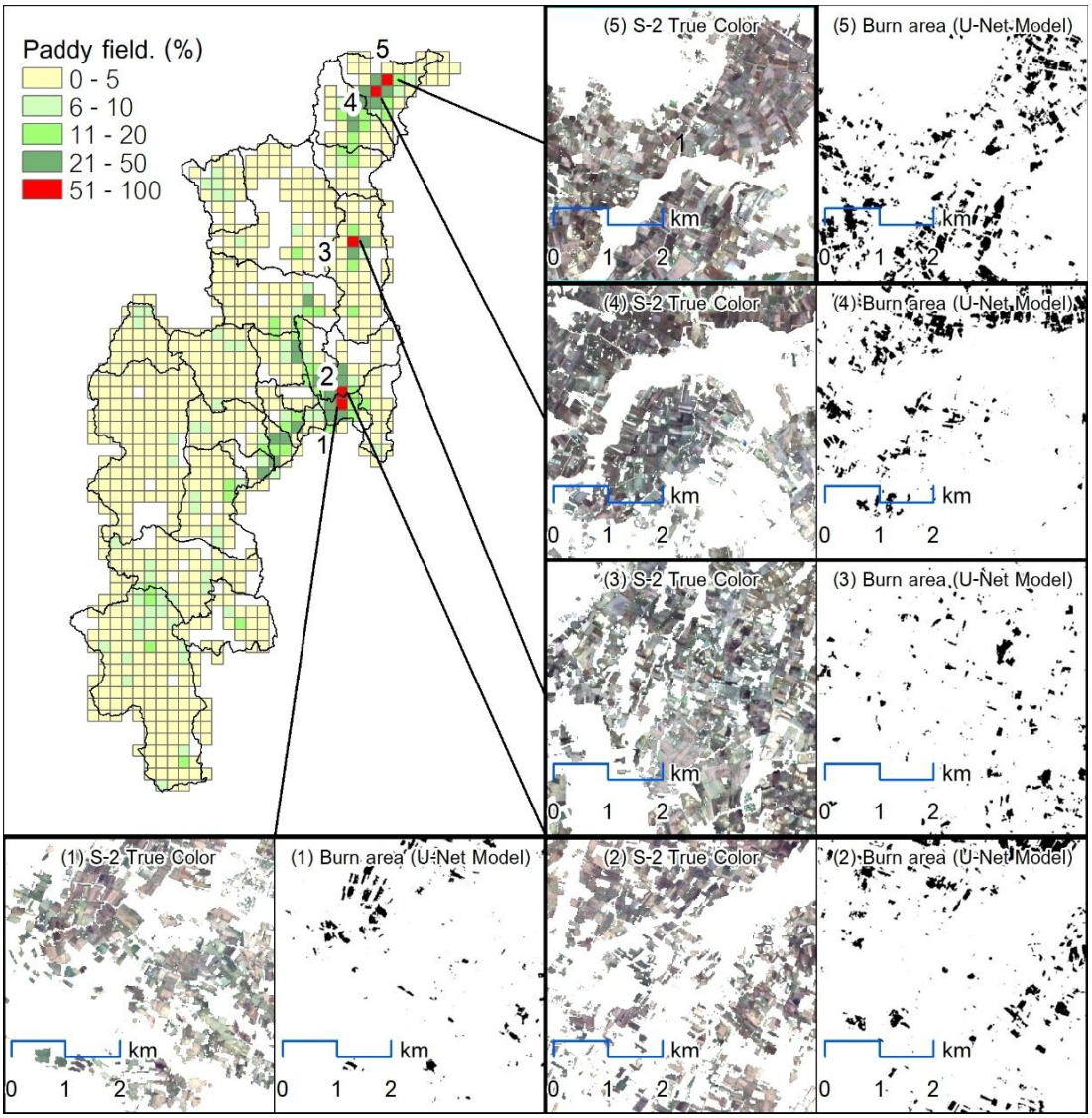

Fig. 5. Locations of the burned area analysis sites where rice paddy density exceeds 50% within Chiang Mai Province, True Color Sentinel-2 imagery acquired on 24 December 2024, and the burned area classification results generated by the U-Net deep learning model.

Regarding the spatial analysis results of burned areas were evaluated using a threshold value ≤ 50 (black color). The results indicate that the proportion of burned pixels accounted for 9.952% of the total image area, equivalent to approximately 2.4880 km². The cultivated region covered 52.441% of the total image area, corresponding to approximately 13.1102 km². Within the cultivated region, burned areas accounted for 18.937%, equivalent to approximately 2.4826 km². These findings illustrate the spatial distribution and extent of burned areas within agricultural fields, highlighting the direct impact of agricultural burning activities on cultivated land, as shown in **Fig. 5**.

5. DISCUSSION

These findings are consistent with previous studies highlighting the potential of Convolutional Neural Network (CNN) models for burned area classification using Sentinel-2 imagery. For example, Tonbul et al. (2023) reported an overall accuracy of 97.53% and demonstrated that deep learning models outperform traditional machine learning approaches. However, the study by Tonbul et al. (2023) utilized multispectral data and spectral indices as input variables. In contrast, the present study demonstrates that even when using only RGB imagery, the model is still capable of effectively learning the spatial characteristics associated with burned area patterns.

When considered together with the study of Samphutthanont (2024), which applied the dNBR index derived from Sentinel-2 imagery to detect small burned areas in rice fields that were not captured by conventional hotspot datasets, the present research further advances the methodology by using dNBR results with a threshold adapted to rice field conditions (dNBR ≥ 0.1) as reference data for training the deep learning model. This approach reflects an integration of spectral index-based analysis and deep learning techniques, representing a transition from traditional rule-based processing toward data-driven learning methods.

Furthermore, when compared with the approach proposed by Pinto et al. (2021), which integrates Sentinel-2 imagery with VIIRS hotspot data to improve temporal completeness, that method is particularly suitable for monitoring large-scale fires at the regional level. However, such approaches may still face limitations in detecting small and fragmented agricultural burned areas, particularly rice residue burning in small-scale rice paddy fields. In contrast, the findings of this study suggest that deep learning approaches may offer greater potential for detecting small burned patches at the field scale, where coarse-resolution hotspot datasets (250–1000 m) are limited in their ability to capture such small burning events.

Regarding model generalization, the use of a spatial hold-out data splitting strategy helps reduce spatial leakage and improves the reliability of model evaluation. This approach is consistent with the recommendations of Anand et al. (2024, 2025), who emphasized the importance of domain adaptation when applying deep learning models to new geographic contexts.

The spatial analysis results indicate that burned areas accounted for 9.952% of the total image area and 18.937% within cultivated regions. These findings are consistent with previous evidence showing that agricultural residue burning plays a significant role in contributing to PM2.5 pollution in Chiang Mai (Junpen et al., 2018; Kamton et al., 2019; Jarernwong et al., 2023; Khamkaew et al., 2016). This study demonstrates a methodological progression from spectral index-based analysis (Samphutthanont, 2024) to deep learning approaches applied to RGB satellite imagery, highlighting the strong potential of such methods for operational monitoring of agricultural burning and supporting effective PM2.5 management at the local scale.

However, several limitations should be acknowledged. First, the dataset size remains relatively limited, consisting of a finite number of image patches derived from selected study areas, which may contribute to the high accuracy observed. Second, the use of masked rice cultivation areas, while beneficial for reducing noise, may reduce classification complexity and limit the model's applicability to more heterogeneous landscapes. Third, the presence of smoke during active burning events may obscure surface features in optical imagery, potentially affecting detection accuracy, and was not explicitly addressed in the current model. Another important limitation relates to the temporal dynamics of agricultural burning. In rice cultivation systems, burned surfaces may change rapidly after burning due to plowing, irrigation, vegetation regrowth, or post-harvest land preparation

activities. As a result, burn scars may only remain detectable for a short period of time. Since this study primarily relied on satellite imagery acquired during specific observation periods, some short-duration burning events may not have been fully captured. Incorporating multi-temporal satellite observations could improve the ability to monitor the temporal evolution of agricultural burning and enhance detection reliability.

Overall, the high model performance may partly reflect the simplified classification conditions introduced by masking and homogeneous land cover characteristics. Consequently, the model may require further validation in more complex and heterogeneous environments to ensure its robustness and generalizability.

Future work in this study should explore multi-temporal data integration, cross-regional validation, and the incorporation of atmospheric correction and smoke-robust preprocessing techniques to enhance model performance under varying environmental conditions, particularly in the presence of haze and smoke.

6. CONCLUSIONS

This study developed an integrated approach combining spectral index analysis (dNBR) and deep learning applied to true color satellite imagery to systematically detect agricultural burned areas in Chiang Mai Province, Thailand. The developed U-Net model demonstrated high precision and training stability in detecting small burned areas from true color (RGB) satellite imagery and exhibited stable training performance. In addition, the model showed good generalization capability when applied to new areas, indicating its robustness for operational applications.

Spatial analysis revealed that burned areas were distributed as small fragmented patches within cultivated fields, with a substantial proportion of burned areas occurring within agricultural zones. These findings highlight the important role of agricultural burning in contributing to local PM2.5 concentrations. In conclusion, the application of deep learning techniques to true color satellite imagery provides an effective approach for detecting agricultural burned areas at the field scale. This method offers significant potential as a practical tool for supporting air quality management and haze mitigation, particularly in Chiang Mai Province and other agricultural regions with similar environmental and land-use characteristics.

ACKNOWLEDGEMENT

The authors gratefully acknowledge the financial support provided by the Local Development Project, Chiang Mai Rajabhat University, for the 2025 Fiscal Year. Furthermore, sincere appreciation is extended to AiroTEC, Chiang Mai Rajabhat University, for their assistance and facilities. Their contribution has been instrumental to the successful completion of this research project and the preparation of this research article.

REFERENCES

Anand, A., Imasu, R., Dhaka, S. K., & Patra, P. (2024). Domain adaptation of deep learning segmentation model of small agricultural burn area detection using high-resolution Sentinel-2 observations: A case study of Punjab, India. Preprints. https://doi.org/10.20944/preprints202409.0333.v1

Anand, A., Imasu, R., Dhaka, S., & Patra, P. K. (2025). Domain adaptation and fine-tuning of a deep learning segmentation model of small agricultural burn area detection using high-resolution Sentinel-2 observations: A case study of Punjab, India. Preprints. https://doi.org/10.20944/preprints202501.0563.v1

Andreae, M. O. (2019). Emission of trace gases and aerosols from biomass burning: An updated assessment. Atmospheric Chemistry and Physics, 19(13), 8523–8546. https://doi.org/10.5194/acp-19-8523-2019

Chen, R., Little, R., Mihaylova, L., Delahay, R., & Cox, R. (2019). Wildlife surveillance using deep learning methods. Ecology and Evolution, 9(16), 9453–9466. https://doi.org/10.1002/ece3.5410

Chuvieco, E., & Stoyanov, B. (2023). Global and continental burned area detection from remote sensing: The FireCCI products. In EGU General Assembly 2023.

Filipponi, F. (2018). BAIS2: Burned area index for Sentinel-2. Proceedings, 2(7), 364. https://doi.org/10.3390/ecrs-2-05177

Fornacca, D., Ye, Y., Li, X., & Xiao, W. (2025). Including small fires in global historical burned area products: Promising results from a Landsat-based product. Fire, 8, 422. https://doi.org/10.3390/fire8110422

Giglio, L., Boschetti, L., Roy, D. P., Humber, M. L., & Justice, C. O. (2018). The Collection 6 MODIS burned area mapping algorithm and product. Remote Sensing of Environment, 217, 72–85. https://doi.org/10.1016/j.rse.2018.08.005

Hu, X., Ban, Y., & Nascetti, A. (2021). Uni-temporal multispectral imagery for burned area mapping with deep learning. Remote Sensing, 13(8), 1509. https://doi.org/10.3390/rs13081509

Jarernwong, K., Gheewala, S. H., & Sampattagul, S. (2023). Health impact related to ambient particulate matter exposure as a spatial health risk map: A case study in Chiang Mai, Thailand. Atmosphere, 14(2), 261. https://doi.org/10.3390/atmos14020261

Junpen, A., Pansuk, J., Kamnoet, O., Cheewaphongphan, P., & Garivait, S. (2018). Emission of air pollutants from rice residue open burning in Thailand. Atmosphere, 9(11), 449. https://doi.org/10.3390/atmos9110449

Kamton, R., Satienperakul, K., Yotapakdee, T., & Nunthasen, K. (2019). Haze-related air pollution and impacts on health in Chiang Mai Province. Interdisciplinary Research Journal: Graduate Studies Edition, 8(1), 1–15.

Key, C. H., & Benson, N. C. (2004). Landscape assessment (LA): Sampling and analysis methods (FIREMON Landscape Assessment V4). U.S. Department of Agriculture, Forest Service, Rocky Mountain Research Station.

Khamkaew, C., Chantara, S., & Wiriya, W. (2016). Atmospheric PM2.5 and its elemental composition from near-source and receptor sites during open burning season in Chiang Mai, Thailand. International Journal of Environmental Science and Development, 7(6), 436–440. https://doi.org/10.7763/IJESD.2016.V7.815

Knopp, L. (2021). Development of a burned area processor based on Sentinel-2 data using deep learning. Photogrammetrie–Fernerkundung–Geoinformation, 89, 357–358. https://doi.org/10.1007/s41064-021-00177-6

Knopp, L., Wieland, M., Rättich, M., & Martinis, S. (2020). A deep learning approach for burned area segmentation with Sentinel-2 data. Remote Sensing, 12(15), 2422. https://doi.org/10.3390/rs12152422

Long, J., Shelhamer, E., & Darrell, T. (2015). Fully convolutional networks for semantic segmentation. In Proceedings of the IEEE Conference on Computer Vision and Pattern Recognition (CVPR) (pp. 3431–3440). IEEE. https://doi.org/10.1109/CVPR.2015.7298965

Ma, L., Liu, Y., Zhang, X., Ye, Y., Yin, G., & Johnson, B. A. (2019). Deep learning in remote sensing applications: A meta-analysis and review. ISPRS Journal of Photogrammetry and Remote Sensing, 152, 166–177. https://doi.org/10.1016/j.isprsjprs.2019.04.015

Martins, V. S., Roy, D. P., Huang, H., Boschetti, L., Zhang, H. K., & Yan, L. (2022). Deep learning high resolution burned area mapping by transfer learning from Landsat-8 to PlanetScope. Remote Sensing of Environment, 280, 113203. https://doi.org/10.1016/j.rse.2022.113203

Miller, J. D., & Thode, A. E. (2007). Quantifying burn severity in a heterogeneous landscape with a relative version of the delta normalized burn ratio (dNBR). Remote Sensing of Environment, 109(1), 66–80. https://doi.org/10.1016/j.rse.2006.12.006

Office of the Permanent Secretary for Agriculture and Cooperatives, Chiang Mai Province. (2026). Basic information of Chiang Mai Province. https://www.opsmoac.go.th/chiangmai-dwl-files-481891791113

Pinto, M. M., Trigo, R. M., Trigo, I. F., & DaCamara, C. C. (2021). A practical method for high-resolution burned area monitoring using Sentinel-2 and VIIRS. Remote Sensing, 13(9), 1608. https://doi.org/10.3390/rs13091608

Reid, J. S., Hyer, E. J., Johnson, R. S., Holben, B. N., Yokelson, R. J., Zhang, J., Campbell, J. R., Christopher, S. A., Di Girolamo, L., Giglio, L., Holz, R. E., Kearney, C., Miettinen, J., Reid, E. A., Turk, F. J., Wang, J., Xian, P., Zhao, G., Balasubramanian, R., … Liew, S. C. (2013). Observing and understanding the Southeast Asian aerosol system by remote sensing: An initial review and analysis for the Seven Southeast Asian Studies (7SEAS) program. Papers in Natural Resources, 443. http://digitalcommons.unl.edu/natrespapers/443

Ronneberger, O., Fischer, P., & Brox, T. (2015). U-Net: Convolutional networks for biomedical image segmentation. In N. Navab, J. Hornegger, W. M. Wells, & A. F. Frangi (Eds.), Medical Image Computing and Computer-Assisted Intervention – MICCAI 2015 (pp. 234–241). Springer. https://doi.org/10.1007/978-3-319-24574-4_28

Roteta, E., Bastarrika, A., Padilla, M., Storm, T., & Chuvieco, E. (2019). Development of a Sentinel-2 burned area algorithm: Generation of a small fire database for sub-Saharan Africa. Remote Sensing of Environment, 222, 1–17. https://doi.org/10.1016/j.rse.2018.12.011

Samphutthanont, R. (2024). Assessing agricultural burned areas using dNBR index from Sentinel-2 satellite data in Chiang Mai, Thailand, from 2019 to 2023. Geographia Technica, 19(2), 46–56. https://doi.org/10.21163/GT_2024.192.04

Schroeder, W., Oliva, P., Giglio, L., & Csiszar, I. A. (2014). The new VIIRS 375 m active fire detection data product: Algorithm description and initial assessment. Remote Sensing of Environment, 143, 85–96. https://doi.org/10.1016/j.rse.2013.12.008

Tonbul, H., Yilmaz, E. O., & Kavzoglu, T. (2023). Comparative analysis of deep learning and machine learning models for burned area estimation using Sentinel-2 image: A case study in Muğla-Bodrum, Turkey. In Proceedings of the 10th International Conference on Recent Advances in Air and Space Technologies (RAST 2023) (pp. 1–5). https://doi.org/10.1109/RAST57548.2023.10197926

van der Werf, G. R., Randerson, J. T., Giglio, L., van Leeuwen, T. T., Chen, Y., Rogers, B. M., Mu, M., van Marle, M. J. E., Morton, D. C., Collatz, G. J., Yokelson, R. J., & Kasibhatla, P. S. (2017). Global fire emissions estimates during 1997–2016. Earth System Science Data, 9, 697–720. https://doi.org/10.5194/essd-9-697-2017

World Health Organization. (2021). WHO global air quality guidelines: Particulate matter (PM2.5 and PM10), ozone, nitrogen dioxide, sulfur dioxide and carbon monoxide. World Health Organization.

Yilmaz, E. O., & Kavzoglu, T. (2024). Burned area detection with Sentinel-2A data: Using deep learning techniques with explainable artificial intelligence. In ISPRS Annals of the Photogrammetry, Remote Sensing and Spatial Information Sciences (Vol. X-5-2024). ISPRS TC V Mid-term Symposium Insight to Foresight via Geospatial Technologies, Manila, Philippines.

Zhu, X. X., Tuia, D., Mou, L., Xia, G.-S., Zhang, L., Xu, F., & Fraundorfer, F. (2017). Deep learning in remote sensing: A comprehensive review and list of resources. IEEE Geoscience and Remote Sensing Magazine, 5(4), 8–36. https://doi.org/10.1109/MGRS.2017.2762307